



# Investigations on the sensitivity of the relationships between sound absorption characteristics and microstructure related parameters for polyurethane foams

Morvan Ouisse, Olivier Doutres, Nouredine Atalla, Mohamed Ichchou, D.  
Begg

## ► To cite this version:

Morvan Ouisse, Olivier Doutres, Nouredine Atalla, Mohamed Ichchou, D. Begg. Investigations on the sensitivity of the relationships between sound absorption characteristics and microstructure related parameters for polyurethane foams. 21st International Congress on Acoustics (ICA 2013), Jan 2013, France. 10.1121/1.4799699 . hal-00993879

**HAL Id: hal-00993879**

**<https://hal.science/hal-00993879>**

Submitted on 20 May 2014

**HAL** is a multi-disciplinary open access archive for the deposit and dissemination of scientific research documents, whether they are published or not. The documents may come from teaching and research institutions in France or abroad, or from public or private research centers.

L'archive ouverte pluridisciplinaire **HAL**, est destinée au dépôt et à la diffusion de documents scientifiques de niveau recherche, publiés ou non, émanant des établissements d'enseignement et de recherche français ou étrangers, des laboratoires publics ou privés.

# Proceedings of Meetings on Acoustics

Volume 19, 2013

<http://acousticalsociety.org/>

**ICA 2013 Montreal**  
**Montreal, Canada**  
**2 - 7 June 2013**

## Structural Acoustics and Vibration

### Session 1pSA: Measurement and Modeling of Structures with Attached Noise Control Materials II

#### 1pSA3. Investigations on the sensitivity of the relationships between sound absorption characteristics and microstructure related parameters for polyurethane foams

Morvan Ouisse\*, Olivier Doutres, Noureddine Atalla, Mohamed Ichchou and David Begg

\*Corresponding author's address: Applied Mechanics, FEMTO-ST, 24 rue de l'épître, 25000, Besançon, France, [morvan.ouisse@univ-fcomte.fr](mailto:morvan.ouisse@univ-fcomte.fr)

Straightforward semi-phenomenological models have been developed for highly porous polyurethane foams to predict the macroscopic non-acoustic parameters involved in the classical Johnson-Champoux-Allard model (i.e., porosity, airflow resistivity...) from microstructure properties (i.e., strut length, strut thickness and reticulation rate). These microstructure properties are measured using sophisticated optical methods (i.e., optical microscope, SEM) and a large variability can be observed due to great complexity of the 3D microstructure; variability which also depends on the precision of the measurement device. This work investigates how the variability associated with the model inputs affects the model outputs (i.e., non-acoustic parameters, surface impedance and sound absorption coefficient). The sensitivity analysis is based on the Fourier Amplitude Sensitivity Test (FAST). It helps quantify the correlation between the input parameters and identify the parameters contributing the most to output variability, thus requiring precise measurement. This study illustrates the preponderant impact of the reticulation rate (i.e., open pore content) on acoustic performances and guides the user on the required optical measurement device.

Published by the Acoustical Society of America through the American Institute of Physics

## INTRODUCTION

Two semi-phenomenological models have been proposed recently to link the microstructure properties of highly porous Polyurethane (PU) foams to their sound absorbing behavior<sup>1,2</sup>. A 3-parameter model<sup>1</sup> was first proposed to link three main microstructure properties of fully and partially reticulated isotropic PU foams (i.e., strut length  $l$ , strut thickness  $t$  and reticulation rate  $R_w$ ) to the macroscopic non-acoustic parameters involved in the classical Johnson-Champoux-Allard (JCA) model<sup>3</sup> (i.e., porosity  $\phi$ , airflow resistivity  $\sigma$ , tortuosity  $\alpha_\infty$ , viscous  $\Lambda$  and thermal  $\Lambda'$  characteristic lengths). This 3-parameter model was based on existing scaling laws, validated for fully reticulated polyurethane foams, and improved using both geometrical and empirical approaches to account for the presence of membrane closing the pores. A 2-parameter model for highly porous PU foam was next proposed<sup>2</sup>. It is a simplification of the 3-parameter model. This model only requires measurements of the cell size  $C_s$  and reticulation rate  $R_w$  assuming that the geometric ratio between strut length  $l$  and strut thickness  $t$  is known. Indeed, considering cell size in place of strut's dimensions considerably simplifies the measurement process and practical use of the model since the cell size parameter is commonly used by chemists.

The two semi-phenomenological models require the challenging task of characterizing the representative unit-cell of such complex and disordered network that constitutes the porous frame. It is performed by direct measurements of the foam microstructure properties from 2D micrographs. Two different optical devices are used and compared in this work; a scanning electron microscope (SEM) and an optical microscope also called stereomicroscope. Electron microscopes have numerous advantages over optical microscopes; they have a higher resolution, a higher magnification and a higher depth of field. However, they have also several disadvantages; they are extremely expensive, the surface of the samples must be coated with a very thin layer of metal (to reflect the electrons) which is difficult to apply for highly porous materials. On the other hand, optical microscopy creates strong light reflections around the polymer struts and on the pores membranes which complicates the microstructure characterization.

The objective of this paper is to investigate how the variability associated with the semi-phenomenological models inputs (i.e., microstructure characterization) affects the models outputs (i.e., non-acoustic parameters, surface impedance and sound absorption coefficient) and give an insight on the required precision of the optical devices. The microstructures of two foams, already investigated in reference<sup>2</sup>, are characterized using both an electron microscope and an optical microscope. One foam is fully reticulated (100% of open pores), and the other one is partially reticulated with only 30% of open pores. Two representative unit cells with their associated standard deviation are thus provided for each of the foams (one for each optical device). A sensitivity analysis based on the Fourier Amplitude Sensitivity Test (FAST) is then performed to investigate the impact of the microstructure characterization.

## MICROSTRUCTURE CHARACTERIZATION

Polyurethane foams have a complex microstructure consisting of an interconnected network of struts forming 3D structures. This structure can be idealized as a packing of truncated octahedron cells (i.e., isotropic tetrakaidecahedron) as shown in Fig. 1. The microstructure characterization consists in the determination of a unit-cell representative of the complex 3D structure. The struts of the representative unit-cell are assumed to be straight, to have a triangular concave cross-section (Plateau border) which remains constant along the strut. The void volume at the strut connections is neglected here; which thus restricts the study to highly porous foams. The properties of the representative unit-cell are: mean cell size  $C_s$  [ $\mu\text{m}$ ], mean strut length  $l$  [ $\mu\text{m}$ ], mean thickness  $t$  [ $\mu\text{m}$ ] and the reticulation rate  $R_w$  [%]. The struts of polyurethane foams having triangular cross-section shape, only the edge  $a$  of the triangle is measured on the micrographs. The strut thickness  $t$  is the height of this triangle assumed equilateral and is thus given by  $t = a\sqrt{3}/2$ . Strut length  $l$  is derived as the mean value between the three lengths  $l_1$ ,  $l_2$ , and  $l_3$  as show in Fig. 1. The reticulation rate  $R_w$  [%], which gives the open window content of the material, is estimated by the ratio of the number of open window to the total number of windows visible on the pictures. The Degree of Anisotropy of the cell (DA) is also estimated. It is defined as the large to small cell radius ratio. All these properties are measured from the 2D micrographs using the "Image J" software. In order to ensure that the characterized unit-cell is representative of a mean cell for each material, all properties and associated expanded uncertainties are determined from a large number of measurements: e.g., 20 measurements for  $C_s$ ,  $t$ , and  $l$ , and approximately 800 windows are counted to estimate  $R_w$ .

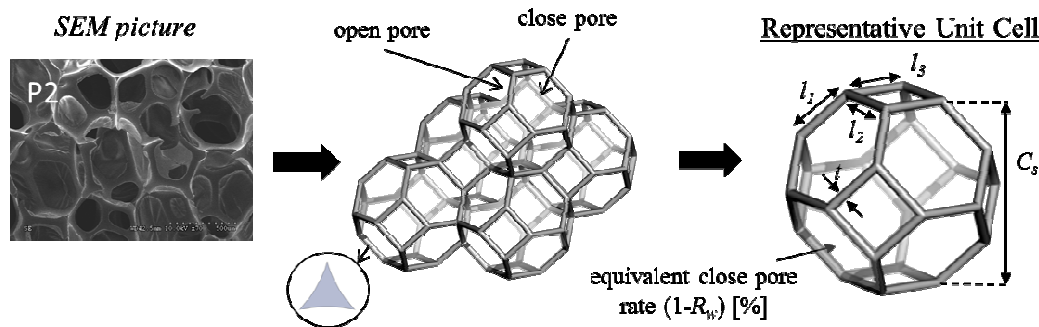


FIGURE 1. Polyurethane foam idealized as a packing of truncated octahedron cells.

The two PU foams investigated in this work are provided by the Woodbridge Group. Foam P1 is a fully reticulated foam with a small cell size ( $C_s \approx 650 \mu\text{m}$ ). Foam P2 is partially reticulated foam with a smaller cell size ( $C_s \approx 600 \mu\text{m}$ ) and a low reticulation rate ( $R_w \approx 30\%$ ). Note that these two foams have already been presented in reference<sup>2</sup>. 2D micrographs are taken using a scanning electron microscope and a stereomicroscope and some samples are presented in Fig. 2. An intermediate magnification is chosen for cell size and ligament length measurements in order to have several cells appearing on the same picture. The magnification is increased for strut thickness measurements. In the case of the SEM characterization, the microstructure properties measurements are carried out on pictures taken in the plane parallel to the wave propagation and in the plane perpendicular to the acoustic wave propagation. Optical micrographs have only been taken in the plane perpendicular to the acoustic wave propagation since the degree of anisotropy (DA) of these two foams is below the discrimination threshold set to  $DA=1.25$ . All the measured microstructure properties are given in Table 1.

TABLE 1. Microstructure properties of the two PU foams.

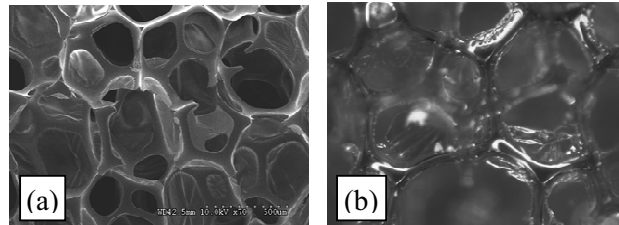
	Material P1		Material P2	
	SEM	Optical	SEM	Optical
$C_s$ ( $\mu\text{m}$ )	673 ( $\pm 35$ )	606 ( $\pm 31$ )	616 ( $\pm 28$ )	640 ( $\pm 22$ )
$l$ ( $\mu\text{m}$ )	208 ( $\pm 16$ )	208 ( $\pm 7$ )	213 ( $\pm 13$ )	211 ( $\pm 11$ )
$t$ ( $\mu\text{m}$ )	46 ( $\pm 3$ )	45 ( $\pm 2$ )	50 ( $\pm 2$ )	40 ( $\pm 3$ )
$R_w$ (%)	100 (-)	-	32 ( $\pm 4$ )	-

Figure 2 shows that the cell contours appear much more clearly on SEM micrographs because of the higher depth of field provided by the electron microscopy. It is thus found that the cell size is more easily estimated on SEM pictures. In order to have a clear visualization of the outside and inside of the cell for cell size measurements, two optical micrographs are taken with two consecutive focal lengths. This technique compensates for the short depth of field provided by the stereomicroscope. Cell size measurements made on optical micrographs are in the same order of magnitude compared with the ones made on SEM micrographs (see Table 1). The measurements variability is also comparable as shown in the histograms presented in Figs. 3(c) and 3(h) and Figs. 4(c) and 4(h).

The variability in strut length measurement is acceptable except for the SEM characterization of the fully reticulated foam P1. The histogram associated to this measurement (see Fig. 3(a)) is divided in two blocks corresponding to the measurements performed on the two sides of the foams (i.e., the two faces parallel and perpendicular to the acoustic wave propagation). Indeed, the cell elongation is more pronounced on the micrographs taken in the plane parallel to the wave propagation and the mean strut length is longer. The strut length variability associated to the SEM characterization procedure is thus greater (as mentioned previously, the characterization procedure carried out from optical micrographs only includes micrographs taken in the plane perpendicular to the acoustic wave propagation). Nevertheless, the mean strut length of material P1 is found identical with the two microscope devices.

Strut thickness measurements carried out on the fully reticulated material P1 are identical for both microscope devices. Surprisingly, the measurement variability is similar even if the resolution of the SEM pictures is higher. The struts of a 75 ppi foam are thus sufficiently thick to make use of an optical microscope. It is worth mentioning that the fully reticulated foam P1 has been reticulated using the thermal method<sup>5</sup> (the membranes are burnt and may stick around the struts). The struts are devoid of residual membranes and thus have very well defined contours which simplify the measurement process. In the case of partially reticulated foams, the SEM technique allows a large color

contrast between struts and membranes as shown in Figs. 2. However, the strut thickness measurements performed from the optical microscope are not straightforward. The contours of the struts are barely visible; especially for the material P2 whose bulk material is almost transparent. Strong light reflections, characteristic of light microscopy and observed in Fig. 2, also complicate the measurement process. All these issues lead to a strut thickness slight underestimation as shown in Table 1.



**FIGURE 2.** Micrographs of partially reticulated PU foam P2: (a) SEM, (b) stereo-microscope.

As mentioned previously, the reticulation rate is determined by the ratio of the number of open window to the total number of windows visible on the micrographs. Most of the time, the distinction is clear between the two kinds of pores. However, when present, the half open pores were considered open. This measurement method is in good agreement with the one used by Zhang *et al.*<sup>6</sup>. Due to its very short depth of field, the optical microscopy is unable to capture all the open and closed pores (see Fig. 2(b)): it should not be used to measure  $R_w$ . It is worth mentioning that some PU foams investigated in references<sup>1,2</sup> depict an anisotropy in the reticulation rate: i.e., a different reticulation rate is observed in the longitudinal direction (SEM pictures taken in the plane perpendicular to the wave propagation) and in the transverse direction (SEM pictures taken in the plane parallel to the wave propagation). However, this reticulation anisotropy is not observed for foam P2 which is characterized by a reticulation rate around 30% in both directions.

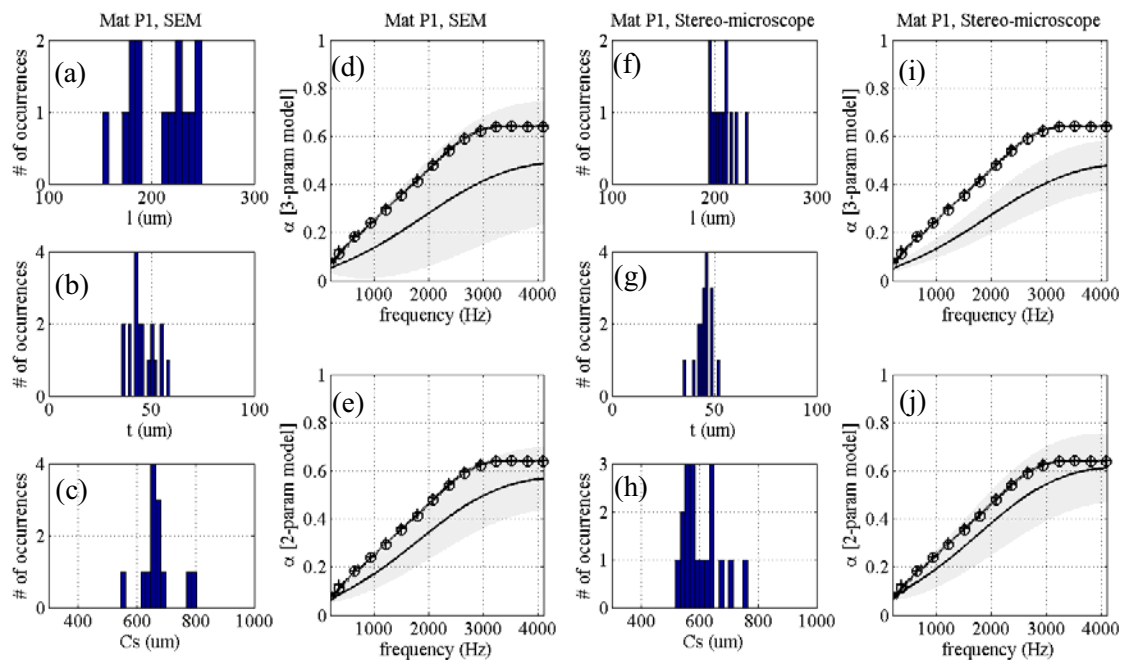


**FIGURE 3.** Fully reticulated material P1; SEM characterization: (a)-(c) Histograms of the inputs and sound absorption coefficients derived with both (d) the 3-parameter and (e) the 2-parameter models; Stereomicroscope characterization: (f)-(h) Histograms of the inputs and sound absorption coefficients derived with both (i) the 3-parameter and (j) the 2-parameter models. (grey area) propagation of non-acoustic measurement uncertainties; (O,+) impedance tube measurements (test of two different samples)

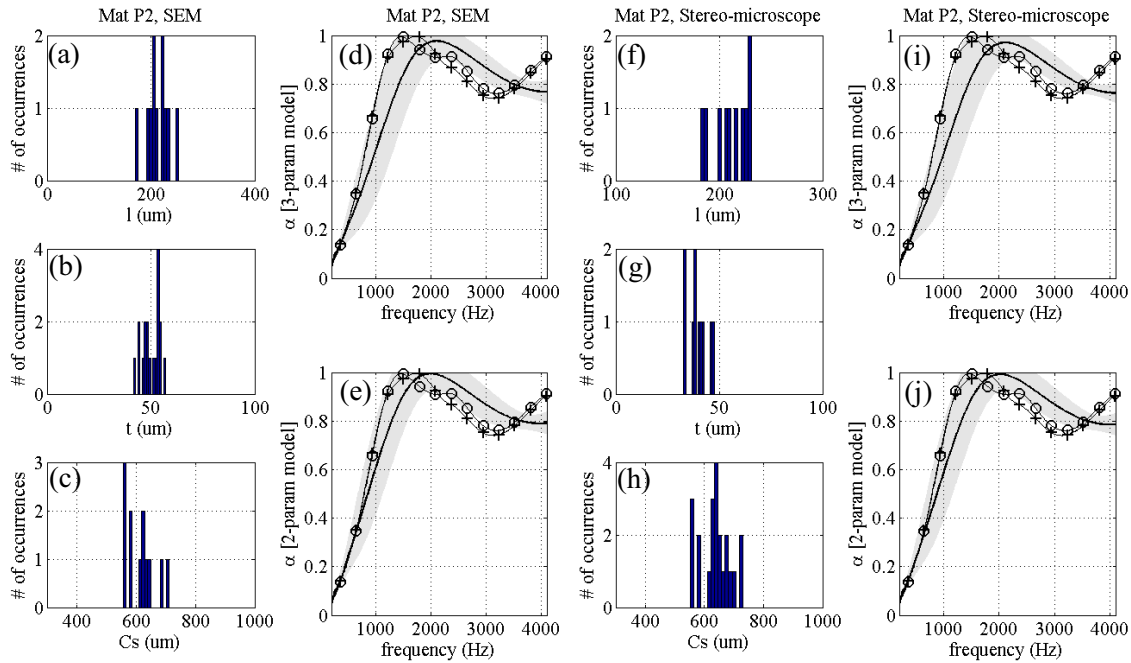


**FIGURE 4.** Partially reticulated material P2; SEM characterization: (a)-(c) Histograms of the inputs and sound absorption coefficients derived with both (d) the 3-parameter and (e) the 2-parameter models; Stereomicroscope characterization: (f)-(h) Histograms of the inputs and sound absorption coefficients derived with both (i) the 3-parameter and (j) the 2-parameter models. (grey area) propagation of non-acoustic measurement uncertainties; (O,+) impedance tube measurements (test of two different samples)

## SEMI-PHENOMENOLOGICAL MODELS

The two semi-phenomenological models are briefly recalled in this section. The links between microstructure and the non-acoustic properties are derived using a combination of geometrical calculations on the representative unit-cell and augmented scaling laws based on an empirical approach to account for the presence of closed pores<sup>1,2</sup>. In the case of the 3-parameter model<sup>1</sup>, the micro-macro links are written in terms of strut length  $l$ , strut thickness  $t$  and reticulation rate  $R_w$  such as:

$$\begin{aligned}
 \phi &= 1 - C_t^p \left( \frac{t}{l} \right)^2, \\
 \Lambda' &= \frac{2V_f}{A_s + (1 - R_w)A_w}, \\
 \sigma &= C^\beta \left( C_r^p \frac{t}{l^2} \right)^2 \left( \frac{1}{R_w} \right)^{1.1166}, \\
 \alpha_\infty &= 1.05 \left( \frac{1}{R_w} \right)^{0.3802}, \\
 \Lambda &= \frac{\Lambda'}{n}, \text{ with } n = 1.55 \left( \frac{1}{R_w} \right)^{0.6763},
 \end{aligned} \tag{1}$$

with  $C_t^p = (2\sqrt{3}-\pi)/\sqrt{2}$ ,  $V_f$  the cell volume,  $A_s$  the surface of the struts and  $A_w$  the total surface of the pores weighted here by the closed pore content  $(1-R_w)$ ,  $C_r^p = 3\pi/8\sqrt{2}$ ,  $C^\beta = 128\eta$  and  $\eta$  the viscosity of air.

In the case of highly porous PU foams, simple relations have been found between strut dimensions and cell size. The strut length  $l$  is approximately equal to  $l = C_s/A\sqrt{2}$  with  $A = 2.33 \pm 0.36$  which is very close to the theoretical value of  $A=2$  for an idealized truncated octahedron (i.e., isotropic tetrakaidecahedron) unit-cell. The strut thickness  $t$  is equal to  $t = l/B$  with  $B = 3.78 \pm 0.53$ . Using these two scaling coefficient the 3-parameter model is simplified to get the 2-parameter model<sup>2</sup> such as:

$$\begin{aligned}\phi &= \phi = 1 - \frac{C_t^p}{B^2}, \\ \Lambda' &= C_s \frac{8(1 - (2\sqrt{3} - \pi)/B^2\sqrt{2})/3A}{(1 + 2\sqrt{3}) - R_w(1 + 2\sqrt{3} - 4\pi/B\sqrt{3})}, \\ \sigma &= C^\beta \left( C_r^p \frac{A\sqrt{2}}{B} \right)^2 \left( \frac{1}{C_s} \right)^2 \left( \frac{1}{R_w} \right)^{1.1166}.\end{aligned}\quad (2)$$

The 2-parameter model only requires measurements of the cell size  $C_s$  and reticulation rate  $R_w$ . This simplification is particularly worthwhile for fully reticulated foams ( $R_w = 100\%$ ) since the microstructure characterization can be performed using an optical microscope. Note that the empirical equations for the tortuosity  $\alpha_\infty$ , and characteristic length ratio  $n$  are not changed in the 2-parameter model since it has been observed in reference<sup>1</sup> that they do not depend on cell size but only on the reticulation rate  $R_w$ .

The estimated non-acoustic properties will be used as inputs in the JCA model to predict the sound absorption coefficients of materials P1 and P2.

## SENSITIVITY ANALYSIS

A so-called global sensitivity analysis method<sup>4</sup> is used. It is able to estimate the sensitivity of a model to large variations of input parameters using a variance decomposition and identify input parameters cross coupling effects. The Fourier Amplitude Sensitivity Test (FAST) is an efficient technique that can be used to estimate the "main effect" (also named first order term) and the "Total Sensitivity Indexes" (TSI)<sup>4</sup>. Indeed, concerning a quantity of interest (the output of the model), the Total Sensitivity Index of parameter  $i$ , denoted by  $TSI(i)$ , is defined as the sum of all the sensitivity indexes (including all the interactions effects) involving parameter  $i$ . For example, suppose that we only have three input parameters, namely  $A$ ,  $B$  and  $C$  in our model. The total effect of parameter  $A$  on the output is  $TSI(A) = SI(A) + SI(AB) + SI(AC) + SI(ABC)$ . Here,  $SI(A)$  denotes the first order sensitivity index for parameter  $A$ ,  $SI(AX)$  is the second order sensitivity index for the parameter  $A$  and  $X$  (for  $X \neq A$ ), i.e. the interaction between parameters  $A$  and  $X$ , and so on. The first order sensitivity index does not take into account coupling effects between parameters, but considers variation of the parameter according to its statistical distribution on a possibly large range. All indexes can be estimated using variance decomposition methods, which are most of the time based on random samplings. The FAST technique uses Fourier transforms associated to specific sampling strategy to estimate the sensitivity indexes<sup>4</sup>. The indexes presented here are normalized to unit, and are presented together with the "Normalized Standard Deviation" (NSD) of the output of interest, namely

$$NSD(y) = \sqrt{\frac{E(y^2) - E(y)^2}{E(y)^2}} \quad (3)$$

where  $E$  is the expected value of  $y$ . This indicator gives information about the global variability of the output of interest.

The sensitivity analysis has been conducted on several cases detailed here, according to input parameters given in table 1. The probability density functions that have been used are uniform for geometric ratios  $A$  and  $B$ , and Gamma laws for all other parameters. The results are illustrated in figure 5.

- a) Material P1 characterized with SEM has been first investigated. In a first step, the 3-parameter model has been used with a reticulation rate of 100%. The sensitivity analysis is then performed using 2

parameters, namely the strut length  $l$  and thickness  $t$ . The results are in Fig. 5(a). The porosity is almost insensitive to input parameters, so the computed sensitivity indexes have little physical sense. This is not the case concerning flow resistivity, whose value is very much impacted by the input parameters, and more precisely by the strut length that captures around 80% of its sensitivity. This is the key parameter for tuning the flow resistivity according to this model when applied to material P1. Only very low coupling effects between input parameters are observed, this is the case for all analyses performed in this work, since TSIs are always very close to SIs. This is a very good point for the model since it indicates that optimizations can be performed on individual parameters to improve the efficiency of the material without any risk related to unexpected coupling effects. Tortuosity is not affected by the input parameters since it depends only on the reticulation rate. On the opposite, both characteristic lengths vary with input parameters, and their values are mainly driven by the strut length (almost 80% of its sensitivity). Finally, for the three sensitive outputs of interest (flow resistivity and characteristic lengths), it appears that the strut length drives the highest part of the variations. The sensibility analysis confirms that even a slight cell anisotropy has noticeable effect on the strut length measurement variability and thus on the non-acoustic parameter identification. It also causes large uncertainty on the sound absorption coefficient as shown in Fig. 3(d).

- b) The sensitivity analysis for Material P1 characterized with the optical microscope (OM), using the 3 parameter model with a reticulation rate of 100%, is shown in Fig. 5(b). The results of the analysis are very close to those obtained with the SEM, except that the strut length sensitivity index is around 60% for flow resistivity and characteristic lengths. The reduced variability on strut length compared to the previous analysis explains this reduction of the impact of  $l$  on the outputs of interest. This is confirmed by the lowest NSD values that can be observed on flow resistivity and characteristic lengths.
- c) Sensitivity analysis for the partially reticulated material P2 characterized with SEM, analyzed using the 3-parameters model, is shown in Fig 5(c). The porosity remains insensitive to input parameters regarding the considered bounds. Flow resistivity exhibits a behavior very close to the one observed in case (a), since the reticulation rate has very little impact on its value: strut length explains the largest part (75%) of the variability. Tortuosity is obviously directly related to reticulation rate. Major changes compared with the fully reticulated case are observed on characteristic lengths: viscous characteristic length value mainly depends on strut length (SI $\approx$ 40%) and reticulation rate (SI $\approx$ 60%), while strut thickness has almost no impact on it, except some small coupling effects. Concerning the thermal characteristic length strut length explains more than 90% of its variability, while reticulation rate fulfill the missing part. It is then clear that the strut thickness is a parameter that explains only a very small amount of the variability of the outputs of interest. Hence for material P2 characterized with SEM, the 2-parameter model will be more appropriate.
- d) The 2-parameters model has been applied to material P1 characterized with SEM. The results of the sensitivity analysis are shown in Fig. 5(d). From a statistical point of view, the 2-parameters model can be seen as a 4-parameters one, since geometric ratios A (an estimate of cell size to strut's length ratio) and B (an estimate of strut's length to thickness ratio) are defined as random variables. It is worth noting that these two parameters are not measured for each foam but have been obtained from the microstructure analysis of 15 highly porous PU foams<sup>1,2</sup> ( $97\% < \phi < 99\%$ ) with relatively low bulk density ( $21.5 \text{ kg.m}^{-3} < \rho_1 < 29.5 \text{ kg.m}^{-3}$ ). The variability of these two coefficients is thus large because it accounts for the microstructural variability between 15 foams. These two coefficients have nevertheless been included in the sensitivity analysis performed here. The results must be balanced by the fact that A and B exhibit high variability due to the fact that they have been determined using a large set of foams. Since P1 is fully reticulated, the analysis considers 3 parameters (A, B and cell size  $C_s$ ). Porosity and tortuosity do not vary, like observed in previous analyses. Flow resistivity, viscous and thermal lengths exhibit the same trends: the three parameters have equivalent impact on the outputs, which indicates that they require the same attention for identification. It is worth noting that measurement variability due to cell anisotropy is less pronounced for the cell size than the strut length presented in case (a). This tends to promote the 2-parameter model (associated to cell size measurements) for estimating the non-acoustic properties of slightly anisotropic foams (i.e.,  $DA < 1.25$ ). Indeed, the variability on the estimated sound absorption is reduced (see Fig. 3(e)) and the agreement between sound absorption measurements and estimates is improved.
- e) Finally, the sensitivity analysis of the 2-parameters model applied to material P2 characterized with SEM is shown in Fig 5. (d). Flow resistivity is impacted in the same manner by all input parameters. Reticulation rate explains more than 50% of the variability observed on the viscous length, while the



other part is due to cell size and geometric ratio A. Moreover, these two parameters are controlling the thermal characteristic length.

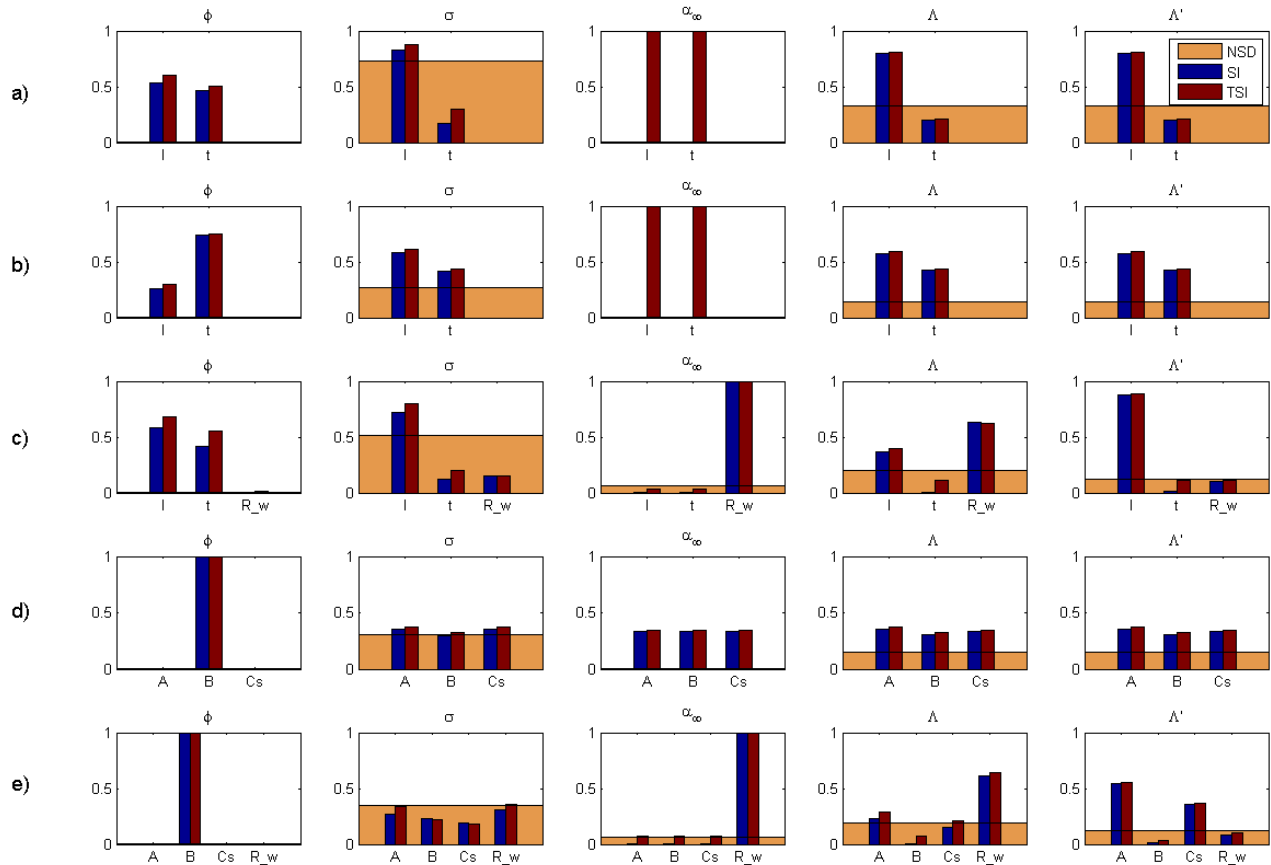


Fig. 5: Results of sensitivity analysis in terms of normalized standard deviations (NSD), first-order sensitivity indexes (SI) and total sensitivity indexes (TSI) of outputs of interest (porosity, flow resistivity, tortuosity, viscous and thermal characteristic lengths) regarding to input parameters (strut length  $l$ , strut thickness  $t$ , reticulation rate  $R_w$ , geometric ratios  $A$  and  $B$ ). a) P1-SEM case with 3-parameter micro/macro model ( $R_w=100\%$ ); b) P1-OM case with 3-parameter micro/macro model ( $R_w=100\%$ ); c) P2-SEM case with 3-parameter micro/macro model; d) P1-SEM case with 2-parameter micro/macro model ( $R_w=100\%$ ); e) P2-SEM case with 2-parameter micro/macro model;

## CONCLUSION

This paper shows that the microstructure of partially reticulated foams should be characterized using a scanning electron microscope (SEM) since an optical microscope (OM) is unable to capture distinctly all the open and close pores, an important measure of reticulation rate. However, the three other microstructure properties (i.e., strut length, strut thickness and cell size) can be measured with both devices since the associated measurement variability has been found to be in the same order of magnitude. This promotes the use of the stereomicroscope for characterizing fully reticulated PU foams since it is much more affordable compared to SEM.

The SEM technique was used to characterize the degree of anisotropy of two PU foams with micrographs taken on two planes parallel and perpendicular to the cell rise direction. The cell anisotropy was found weak for the two foams ( $DA < 1.25$ ). Still, it has a noticeable effect on the strut length variability measured for the fully reticulated foam P1.

A sensitivity analysis has been proposed to investigate impact of the inputs variability on the outputs of the 2 semi-phenomenological models. It has been found that the flow resistivity, viscous and thermal characteristic lengths were the most impacted by measurement uncertainties. In the case of the 3-parameter model, the strut length measurement has been found to have a major impact; and particularly when the measurement variability is large due to cell anisotropy (e.g., material P1). In this case, the 2-parameters model can be pertinent since (i) it avoids the

measurement of the strut length and thickness and (ii) the cell size measurement variability is less impacted by foam anisotropy compared to strut length measurement.

## ACKNOWLEDGMENTS

The authors would like to thank the National Sciences and Engineering Research Council of Canada (NSERC) for providing financial support. This work was co-financed by The French National Research Agency under grant ANR-12-JS09-008-COVIA.

## REFERENCES

1. O. Doutres, N. Atalla and K. Dong, "Effect of the microstructure closed pore content on the acoustic behavior of polyurethane foams", *J. App. Phys.* **110**(6), 064901 (2011).
2. O. Doutres, N. Atalla and K. Dong, "A semi-phenomenological model to predict the acoustic behavior of fully and partially reticulated polyurethane foams", accepted for publication in *J. App. Phys.*, (2013)
3. J.F. Allard and N. Atalla, "Propagation of sound in porous media: Modeling sound absorbing materials", 2nd edition. John Wiley & Sons Ltd, New York (2009).
4. M. Ouisse, M. Ichchou, S. Chedly and M. Collet, "On the sensitivity analysis of porous material models", *J. of Sound and Vib.* **331**, 5292–5308 (2012).
5. O. Doutres, N. Atalla, M. Brouillette and C. Hébert, "Improving the sound absorbing efficiency of closed-cell foams using shock waves", 21<sup>th</sup> ICA, Montreal, 2-7 June (2013).
6. C. Zhang, J. Li, Z. Hu, F. Zhu and Y. Huang, "Correlation between the acoustic and porous cell morphology of polyurethane foam: Effect of interconnected porosity", *Materials and Design* **41**, 319-325 (2012).
7. Anonymous, "Acoustics - Determination of sound absorption coefficient and impedance in impedance tubes. Part 2: Transfer-function method," International Standard ISO-10534-2 (1998).